

Communication

Mechanistic Details of the Titanium-Mediated Polycondensation Reaction of Polyesters: A DFT Study

Zhenyu Guan ^{1,2,3} , Jialong Zhang ³, Wenle Zhou ³, Youcai Zhu ⁴, Zhen Liu ^{4,*} , Yumei Zhang ^{1,2,*} and Yue Zhang ^{1,2}

¹ State Key Laboratory for Modification of Chemical Fibbers and Polymer Materials, Donghua University, Shanghai 201620, China; guanzhy.sshy@sinopec.com (Z.G.); zhangyue@dhu.edu.cn (Y.Z.)

² College of Materials Science and Engineering, Donghua University, Shanghai 201620, China

³ Shanghai Research Institute of Petrochemical Technology, Shanghai 201208, China; zhangjialong.sshy@sinopec.com (J.Z.); zhouwl.sshy@sinopec.com (W.Z.)

⁴ School of Chemical Engineering, East China University of Science and Technology, Shanghai 200237, China; y30200074@mail.ecust.edu.cn

* Correspondence: liuzhen@ecust.edu.cn (Z.L.); zhangym@dhu.edu.cn (Y.Z.)

Abstract: In this work, the mechanism of polyester polycondensation catalysed by titanium catalysts was investigated using density functional theory (DFT). Three polyester polycondensation reaction mechanisms, including the Lewis acid mechanism (M1), the coordination of the ester alkoxy oxygen mechanism (M2) and the coordination of the carboxy oxygen mechanism (M3), were investigated. Three reaction mechanisms for the polycondensation reaction of diethyl terephthalate (DET) were investigated using $\text{Ti}(\text{OEt})_4$ and cationic $\text{Ti}(\text{OEt})_3^+$ as the catalyst. The results show that the polycondensation reaction of the Lewis acid mechanism exhibits similar energy barriers to the catalyst-free condition (42.6 kcal/mol vs. 47.6 kcal/mol). Mechanism M3 gives the lowest energy barrier of 17.5 kcal/mol, indicating that $\text{Ti}(\text{OEt})_4$ is the active centre for the polycondensation reaction. The catalytic efficiency of $\text{Ti}(\text{OEt})_3^+$ is lower than that of $\text{Ti}(\text{OEt})_4$ catalysts due to its higher DET distortion energy (67.6 kcal/mol vs. 37.4 kcal/mol) by distortion–interaction analysis.



Citation: Guan, Z.; Zhang, J.; Zhou, W.; Zhu, Y.; Liu, Z.; Zhang, Y.; Zhang, Y. Mechanistic Details of the Titanium-Mediated

Polycondensation Reaction of Polyesters: A DFT Study. *Catalysts* **2023**, *13*, 1388. <https://doi.org/10.3390/catal13101388>

Academic Editor: Aleksander Filarowski

Received: 24 September 2023

Revised: 17 October 2023

Accepted: 21 October 2023

Published: 23 October 2023



Copyright: © 2023 by the authors. Licensee MDPI, Basel, Switzerland. This article is an open access article distributed under the terms and conditions of the Creative Commons Attribution (CC BY) license (<https://creativecommons.org/licenses/by/4.0/>).

Keywords: polyester polycondensation; titanium catalysts; DFT; reaction mechanism; distortion–interaction analysis

1. Introduction

Polyethylene terephthalate (PET) is one of the most common types of polyester polymer material [1]. PET is widely used in fibres, containers, films, bottles, sheets, plastics and other fields due to its excellent physical, chemical and mechanical properties [2–6]. PET is synthesized by esterification of purified terephthalic acid (PTA) and ethylene glycol (EG), followed by pre-polycondensation and final polycondensation under vacuum conditions [7].

In the synthesis of PET, the catalyst not only influences the reaction rate of the esterification and polycondensation, but also the side reactions during the synthesis process, the reaction selectivity and the properties of the products [8,9]. The catalysts for the polycondensation reaction are of many types [10,11], mainly including antimony, germanium, titanium and aluminium, etc. Antimony catalysts, known for their moderate activity, minimal side reactions and relatively lower thermal degradation efficiency for PET, are the more commonly used than Ge^{4+} , Ti^{4+} and Sn^{4+} catalysts [12]. However, antimony catalysts can be a source of environmental pollution due to their heavy metal content. Therefore, the focus of modern polyester synthesis has been on the development of new polyester catalysts that are efficient, non-toxic and non-polluting [13]. Some degradable co-polyesters, such as poly(butylene succinate) (PBS) and poly(isosorbide-co-ethylene terephthalate) (PEIT), have used titanium catalysts [14,15]. Although Ti-based catalysts are very active relative

to antimony, the first generation of Ti-based catalysts were prone to hydrolysis, reducing activity, and yielded polymers of poor colour. Therefore, a deeper understanding of the mechanism undoubtedly provides a powerful aid for catalyst design.

In recent decades, a very large number of semi-empirical and non-empirical density functionals (DFs) have been developed. This significant progress can be attributed to the fact that DFT achieves a favourable equilibrium between precision and computational expenditure. In light of our previous work [16], the zinc(II) catalyst plays a privileged role in the transesterification reaction of acetoxyaryl and carboxylic acid, by DFT calculation. Meanwhile, the reaction mechanisms of polyester polycondensation and thermal degradation have been widely investigated [11,17,18]. Three polyester polycondensation mechanisms have been proposed (Figure 1). In one, the metal centre of the catalyst acts as a Lewis acid and activates the carbonyl group, causing it to undergo nucleophilic attack in the presence of the alcohol-based oxygen (M1 mechanism, Figure 1a). The exchange reaction of the metal ligand with the OR end group of the oligomer is involved in the other two mechanisms. The alkoxy oxygen atom of the ester is coordinated to the metal centre of the catalyst (M2 mechanism, Figure 1b), or the carbonyl oxygen atom is coordinated to the metal centre (M3 mechanism, Figure 1c). Similar to the Lewis acid polycondensation mechanism, the carbonyl carbon atom is attacked by the alkoxy oxygen atom in the oligomer. The $\text{Ti}(\text{OEt})_4$ catalysed mechanism of the PET polycondensation reaction has been investigated by Shigemoto, and the transesterification reaction of DET with ethanol was used as a model system [11]. The results show that the coordination mechanism of carboxy oxygen exhibits an activation energy of 15.5 kcal/mol, by DFT calculations. The structure and energy of the species in the PET polycondensation reaction can be identified by DFT, and it is confirmed that the high catalytic activity of titanium is not due to the Lewis acid mechanism. Wang reported that a Ti^{4+} tetrahedrally coordinated MOF-catalytic Zr/Ti material can be obtained with an activity close to that of Sb-based polyesters, and also verified by DFT that the reaction obeys the coordination of the carboxy oxygen mechanism [19].

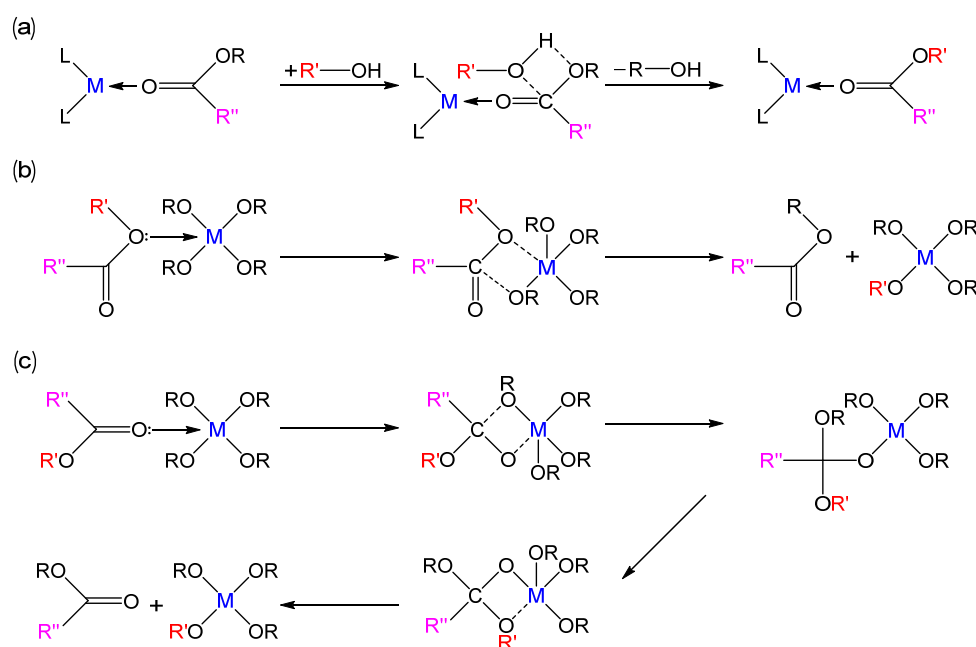


Figure 1. Three polycondensation reaction mechanisms proposed in [11] (copyright 2011, Elsevier). (a) Lewis acid mechanism (M1); (b) coordination of the alkoxy oxygen mechanism (M2); (c) coordination of the carboxy oxygen mechanism (M3).

In addition, some novel titanium catalysts were designed and developed by DFT methods, such as the catalytic synthesis of PEIT from organic acid–base compounds and the catalytic mechanism of titanate esterification of amino-triphenol [20]. The $\text{Ti}(\text{OEt})_4$ and

Ti(OBu)₄ titanate catalysts are the most commonly used catalysts in practical production. In light of our previous work [21], Ti(OEt)₃⁺ cationic catalyst was found to be present in the polyester degradation process. However, the effect of Ti(OEt)₃⁺ cationic catalyst on the polycondensation reaction has not been the subject of further investigation. Furthermore, the possible deactivation of the titanium catalyst during polycondensation is an open question and not fully understood because it was reported that the polymeric form of titanium compounds as products of hydrolysis are still catalytically active [22,23]. There are good reasons to suspect that the interconversion between Ti(OEt)₄ and Ti(OEt)₃⁺ cationic catalysts affects the polycondensation and thermal degradation reactions. Therefore, the role of two titanium catalyst models in the polyester polycondensation reaction was theoretically investigated by using the DFT calculation. The mechanism of catalytic action was elucidated by analysing the structure and energy of the substances involved in the reaction.

2. Results and Discussion

2.1. Polyester Polycondensation Reactions without Catalysts

First, the transesterification reaction of DET with ethanol was investigated as a model system for the catalyst-free polycondensation reaction (Figure 2a). The molecular electrostatic potential (MESP) analysis on the DET molecule shows that the carbonyl oxygen is most likely to be attacked by an electrophile in the polycondensation of polyesters (Figure S1). Frontier orbital theory suggests that a chemical reaction occurs at the location where the highest occupied molecular orbital (HOMO) of one reactant and the lowest unoccupied molecular orbital (LUMO) of the other reactant can produce the greatest overlap. Closer the energies of the HOMO and LUMO involved in the reaction indicate a stronger interaction and a greater stabilization of the system. As shown in Figure 2b, it can be seen that the LUMO of the reactant DET is mainly located in the π bonding orbitals of the benzene ring, while the HOMO of the reactant ethanol is mainly located in the π_{C-O} antibonding orbitals. The HOMO energy of ethanol is -7.6 eV and is -2.1 eV for the LUMO energy in DET, resulting in a HOMO–LUMO energy gap of 5.5 eV.

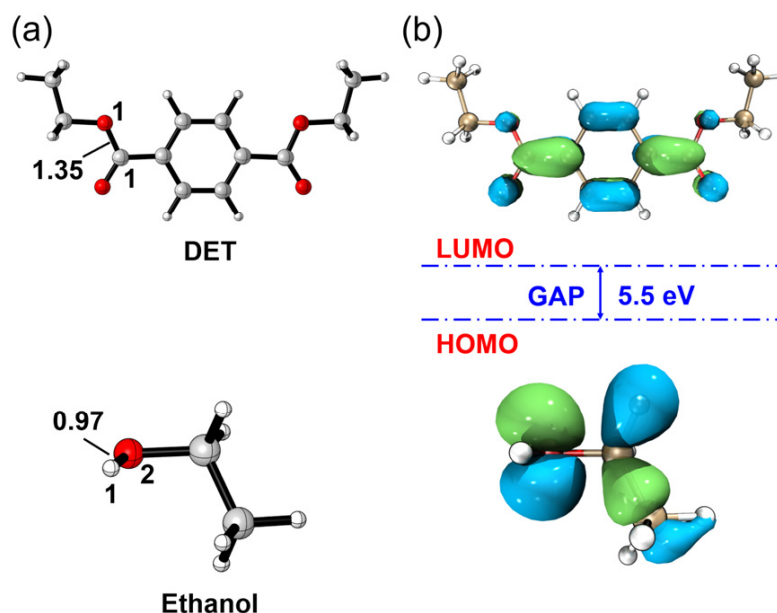


Figure 2. (a) Optimized structures of DET and ethanol; (b) HOMO, LUMO and HOMO–LUMO energy gap.

In this reaction, the O1 atom of ethanol acts as a nucleophilic reagent to attack the carbonyl carbon (C1) atom of DET, resulting in the formation of a cyclic four-centre transition state (Figure 3). The H1 atom of ethanol is simultaneously transferred to the O2 atom of the ester group, and the corresponding product is formed as the C1–O2 bond is cleaved. The

C1–O2 bond extends from 1.35 Å in **Int1** to 1.73 Å in **TS1**, and the bond length of H1–O1 was extended from 0.97 Å to 1.21 Å. In the absence of a catalyst, the energy barrier of the transesterification reaction between DET and ethanol is 47.6 kcal/mol.

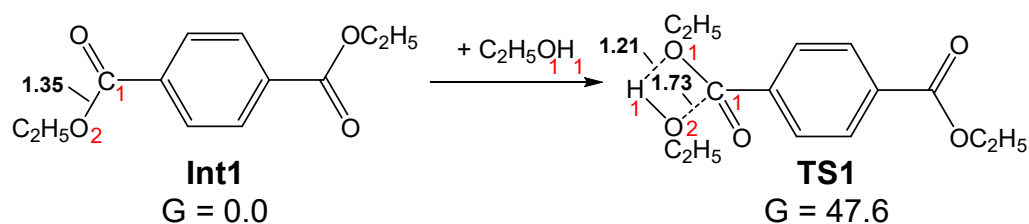


Figure 3. Polyester polycondensation of DET with ethanol under catalyst-free conditions. Energies are in kcal/mol and the bond lengths are in Å.

2.2. Molecular Modelling of Catalysts

The effects of two catalysts on the polyester polycondensation reaction were first investigated, including titanium ethoxylate complex $\text{Ti}(\text{OEt})_4$ and its cationic $\text{Ti}(\text{OEt})_3^+$ (Figure 4). $\text{Ti}(\text{OEt})_4$ is a four-coordinated octahedral structure, whereas $\text{Ti}(\text{OEt})_3^+$ catalyst with a cationic centre is a three-coordinated tetrahedral configuration. There are similar C–O and C–C bond lengths for both catalysts. The Ti–O bond lengths are 1.80 Å and 1.75 Å for $\text{Ti}(\text{OEt})_4$ and $\text{Ti}(\text{OEt})_3^+$ catalysts, respectively.

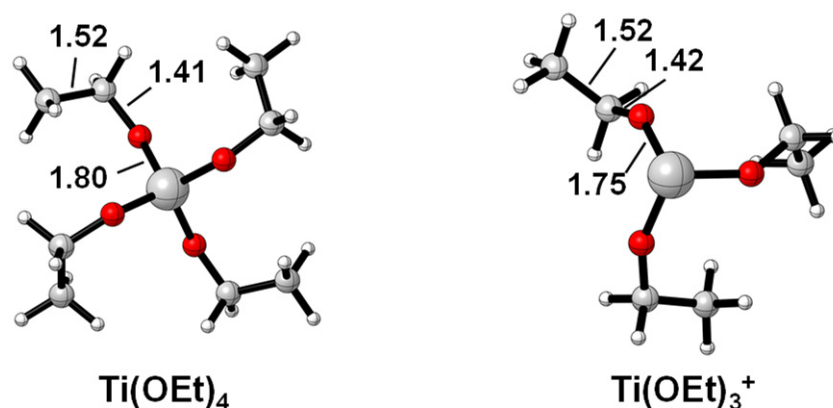


Figure 4. Optimized structure of $\text{Ti}(\text{OEt})_4$ and $\text{Ti}(\text{OEt})_3^+$ catalysts. Bond lengths are in Å.

2.3. Mechanism of Polyester Polycondensation Reaction Catalysed by $\text{Ti}(\text{OEt})_4$

In the M1 mechanism of polyester polycondensation, the product is formed in two steps: (i) the carbonyl oxygen of the reactant DET is coordinated to the metal centre; (ii) the oxygen atom of ethanol acts as a nucleophilic reagent to attack the carbonyl carbon atom of DET, resulting in the formation of a cyclic four-centre transition state (Figure 5). The hydrogen atom of ethanol is simultaneously transferred to the oxygen atom of the ester group, and the corresponding product is formed as the C–O bond is cleaved. The energy barrier of 42.6 kcal/mol must be overcome; this is slightly lower than that in the catalyst-free reaction (47.6 kcal/mol), indicating a slight facilitating effect of the polycondensation reaction in the M1 mechanism using $\text{Ti}(\text{OEt})_4$ as the catalyst.

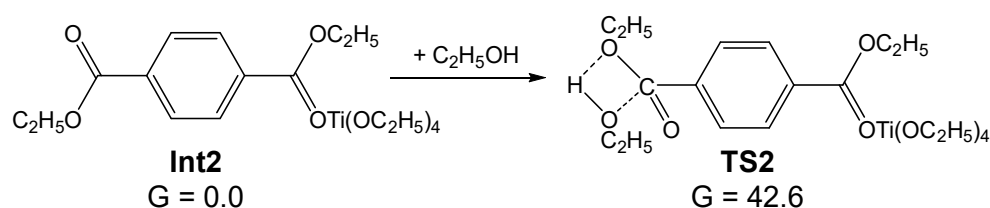


Figure 5. M1 Mechanism for the polyester polycondensation reaction. Energies are in kcal/mol.

Since the M1 mechanism of $\text{Ti}(\text{OEt})_4$ could not effectively reduce the reaction energy barrier for the polyester polycondensation, the M2 and M3 mechanisms were further investigated. As shown in Figure 6, DET weakly coordinates to the $\text{Ti}(\text{OEt})_4$ catalyst with a Ti–O bond length of 3.95 Å. Unlike the catalyst-free reaction, the corresponding product is settled 13.9 kcal/mol below the reference structure **Int3**, indicating that the formation of **Int4** is thermodynamically favourable. The Ti–O1 bond extends from 1.79 Å in **Int3** to 2.10 Å in **TS3**, while the bond length of Ti–O2 has been shortened to 2.04 Å. The energy barrier for the polyester polycondensation reaction of DET catalysed by $\text{Ti}(\text{OEt})_4$ was only 26.8 kcal/mol, which was significantly lower than that of the polyester polycondensation reaction without catalyst (47.6 kcal/mol), indicating that the $\text{Ti}(\text{OEt})_4$ centre promotes the polyester polycondensation reaction following the M2 mechanism.

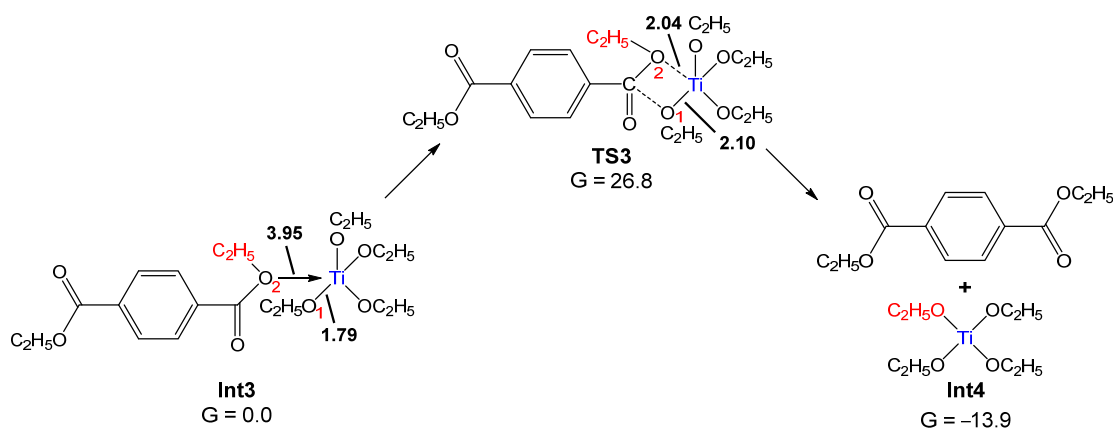


Figure 6. Coordination of the ester alkoxy oxygen mechanism for the polyester polycondensation reaction. Energies are in kcal/mol.

In the M3 mechanism, the carboxy oxygen of the reactant DET is first coordinated to the metal centre. Subsequently, the oxygen atom of the Ti-centred ethoxylate acts as a nucleophilic reagent to attack the carbonyl carbon atom of DET, resulting in the formation of a cyclic four-centre transition state. This step requires overcoming an energy barrier of 17.5 kcal/mol, and then the Ti-centred ethoxylate is transferred into the DET molecule (Figure 7). Finally, the ethoxy group of the DET molecule transfers to the metal centre to complete the catalytic cycle. Similarly, the corresponding product is settled 15.6 kcal/mol below the reference structure **Int2**, indicating that the formation of **Int5** is thermodynamically favourable. It is noteworthy that the total energy barrier to be overcome in the M3 mechanism is only 19.9 kcal/mol, which is lower than in the M1 and M2 mechanisms, indicating that the $\text{Ti}(\text{OEt})_4$ centre has a significant facilitating effect on the polyester polycondensation reaction in the M3 mechanism.

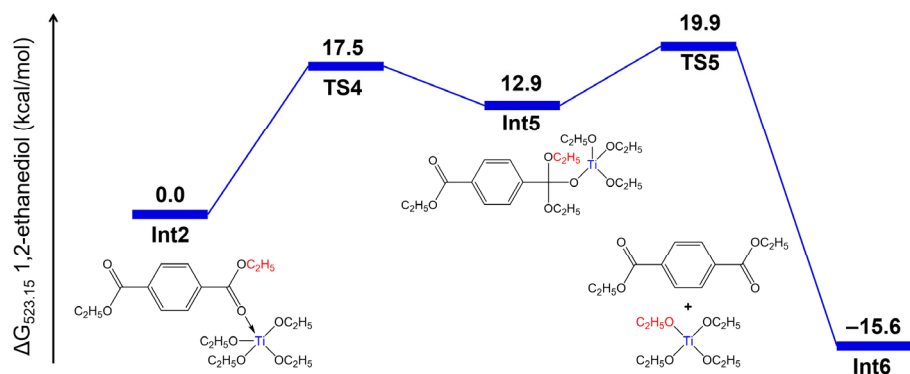


Figure 7. Coordination of the carboxy oxygen mechanism for the polyester polycondensation reaction. Energies are in kcal/mol.

To understand the potential advantages of the M3 mechanism over the $\text{Ti}(\text{OEt})_4$ catalyst, frontier molecular orbital analysis was performed to analyse the stability of the reactants. Figure 8 shows the HOMO, LUMO, and HOMO–LUMO energy gap of intermediates **2** and **3**. The HOMO–LUMO energy gap follows the order $\text{Int3} > \text{Int2}$, indicating that **Int3** has higher chemical stability than **Int2**. Therefore, the energy barrier of the M3 mechanism is more favourable than that of the M2 mechanism due to the unstable reactant.

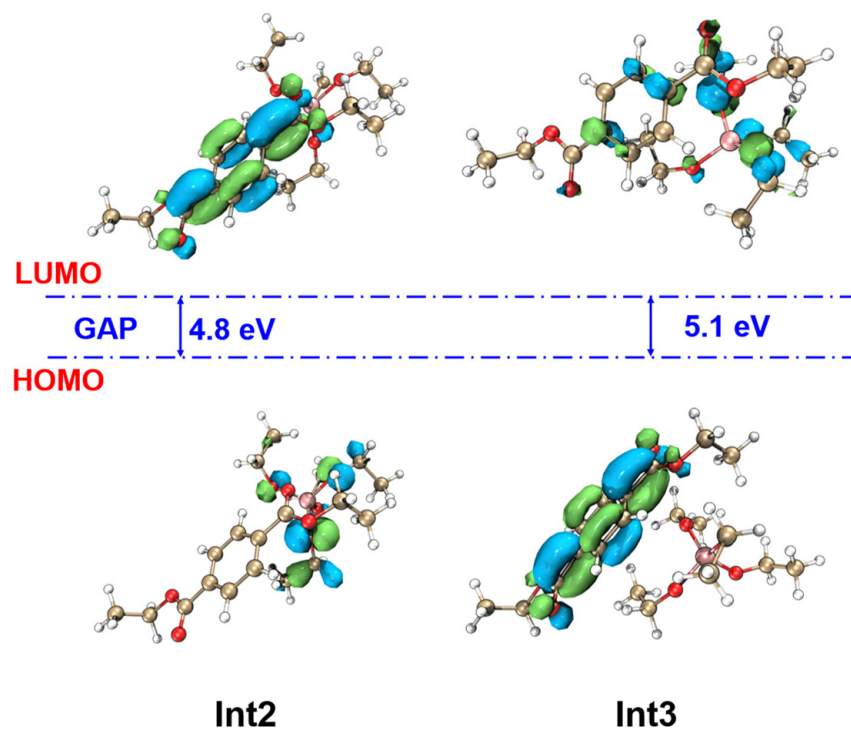


Figure 8. HOMO, LUMO and HOMO–LUMO energy gap for intermediates **2** and **3**.

2.4. Mechanism of Polyester Polycondensation Reaction Catalysed by $\text{Ti}(\text{OEt})_3^+$

In light of our previous work [21], the $\text{Ti}(\text{OEt})_3^+$ cationic catalyst was found to be present in the polyester degradation process when $\text{Ti}(\text{OEt})_4$ was added. The $\text{Ti}(\text{OEt})_3^+$ catalyst may be the active centre of the thermal degradation of polyester and obeys the alkoxide coordination mechanism with a required overcoming energy barrier of 37.3 kcal/mol. To understand the effect of $\text{Ti}(\text{OEt})_3^+$ on the polyester polycondensation reaction, the effect of $\text{Ti}(\text{OEt})_3^+$ on the activation energies of the reaction in the three mechanisms was also investigated. Since the catalyst in the M1 mechanism only acts as a ligand centre and does not actually participate in the transesterification reaction, $\text{Ti}(\text{OEt})_3^+$ did not show a significant promoting effect as with the $\text{Ti}(\text{OEt})_4$ catalyst (Figure 9).

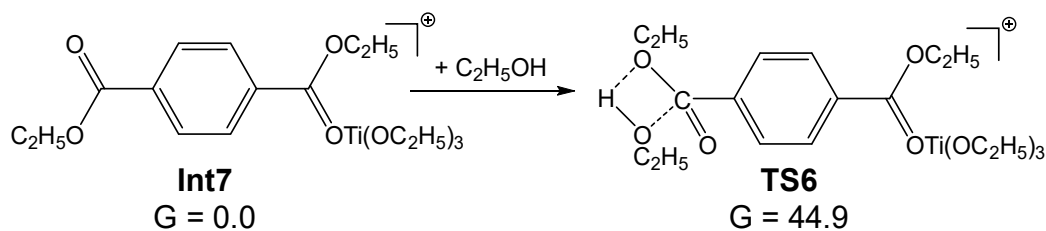


Figure 9. Lewis acid mechanism for the polyester polycondensation reaction over $\text{Ti}(\text{OEt})_3^+$ catalyst. Energies are in kcal/mol.

As shown in Figure 10a, the energy barrier of the M2 mechanism catalysed by $\text{Ti}(\text{OEt})_3^+$ was calculated to be 24.1 kcal/mol, which is significantly lower than that of the polyester

polycondensation reaction without catalyst in Figure 4 (47.6 kcal/mol), indicating that the $\text{Ti}(\text{OEt})_3^+$ centre promotes the polyester polycondensation reaction in the M2 mechanism. The change in bond lengths along the intrinsic reaction coordinate (IRC) is depicted in Figure 10b. The corresponding optimized structures of the reactant, transition state and product are summarized in Figure S2, where the cleavage of the C1–O1 bond in DET and the formation of the C1–O2 bond were selected as the scanned coordinates. The C1–O1 (1.45 Å) on the DET is first broken, and then the C1 atom is bonded with the O2 atom at a distance of 2.11 Å, where the energy barrier reaches the maximum. Subsequently, the energy profile gradually decreases and the corresponding product is formed.

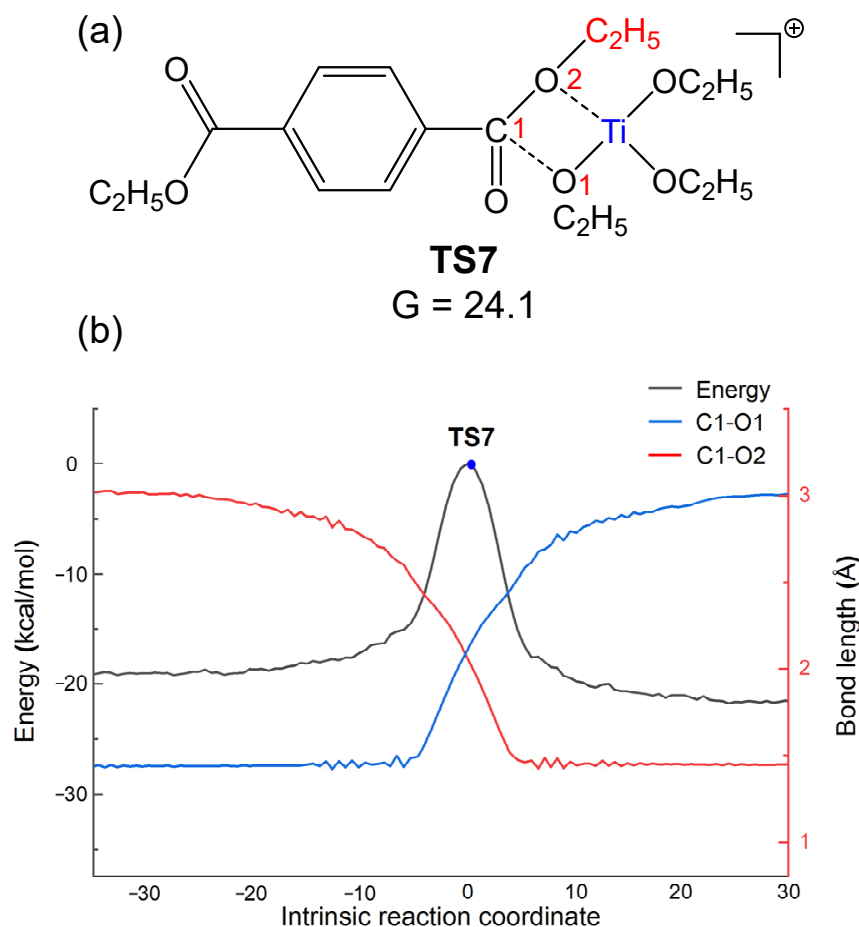


Figure 10. (a) M2 mechanism reaction transition state over $\text{Ti}(\text{OEt})_3^+$ catalyst; (b) bond lengths of key atoms along the intrinsic reaction coordinate.

The molecular structure of $\text{Ti}(\text{OEt})_4$ showed that the reactant EDB could not interact effectively with the titanium centre due to the stable octahedral structure. As shown in Figure 11, the bond length of the Ti–O bond in the three-coordinated $\text{Ti}(\text{OEt})_3^+$ catalyst is 1.98 Å, which exhibits a strong interaction of DET with the catalyst. Subsequently, the oxygen atom of the Ti-centred ethoxylate acts as a nucleophilic reagent to attack the carbonyl carbon atom of DET, resulting in the formation of a cyclic four-centre transition state. This step requires overcoming an energy barrier of 29.4 kcal/mol, and then the Ti-centred ethoxylate is transferred into the DET molecule. Finally, the ethoxy group of the DET molecule transfers to the metal centre to complete the catalytic cycle. Similarly, the corresponding product is settled 0.3 kcal/mol below the reference structure **Int6**, indicating that the formation of **Int9** is thermodynamically favourable.

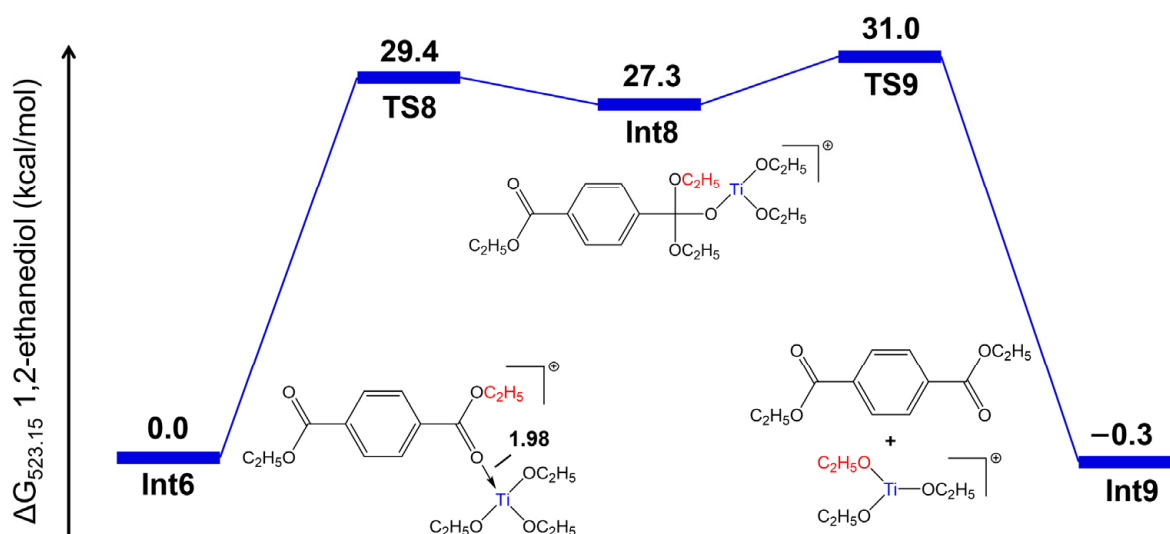


Figure 11. Coordination of the carboxy oxygen mechanism for the polyester polycondensation reaction over $\text{Ti}(\text{OEt})_3^+$ catalyst. Energies are in kcal/mol.

2.5. Comparative Analysis of Reaction Mechanism

The turnover frequency (*TOF*) determines the efficiency of the catalyst. Sebastian [24] proposed that the corresponding *TOF* values can be calculated from the Gibbs free energy transitions in the catalytic reaction path with the following expression:

$$\text{TOF} = \frac{k_B T}{h} \frac{e^{-\Delta G_r^0/RT} - 1}{\sum_{a,b=1}^N e^{(T_a - I_b - \delta G'_{a,b})/RT}} \quad (1)$$

$$\delta G'_{a,b} = \Delta G_r^0 \quad \text{if } a > b \quad (2)$$

$$\delta G'_{a,b} = 0 \quad \text{if } a \leq b \quad (3)$$

where T_a and I_b correspond to the Gibbs free energies of the transition states and intermediates in the reaction path, respectively; ΔG_r^0 is the Gibbs free energy difference between reactants and products in the reaction path. The *TOF* is determined in most cases by one transition state—the *TOF* determining transition state (TDTS), one intermediate—the *TOF* determining intermediate (TDI), and by the reaction energy.

As shown in Table 1, both $\text{Ti}(\text{OEt})_4$ and $\text{Ti}(\text{OEt})_3^+$ catalysts exhibited significant promotion of the polyester polycondensation reaction, with the reaction energy barriers decreasing from 47.6 kcal/mol (Figure 3) under catalyst-free conditions to 19.9 and 24.1 kcal/mol, respectively. The corresponding *TOF* values based on the calculated energies of each reaction pathway were calculated and the results are listed in Table 1. It is clear that $\text{Ti}(\text{OEt})_4$ has the largest *TOF* value of $3.5 \times 10^4 \text{ s}^{-1}$ in the M3 mechanism.

Table 1. Polycondensation reactions and their corresponding Gibbs free energies with different titanium catalysts.

	$\text{Ti}(\text{OEt})_4$			$\text{Ti}(\text{OEt})_3^+$		
	M1 Mechanism	M2 Mechanism	M3 Mechanism	M1 Mechanism	M2 Mechanism	M3 Mechanism
TDI (kcal/mol)	0.0	0.0	0.0	0.0	0.0	0.0
TDTS (kcal/mol)	42.6	26.8	19.9	44.9	24.1	31.0
TOF(s^{-1})	1.3×10^{-5}	47	3.5×10^4	1.4×10^{-6}	630	0.85

In order to understand the differences in the reaction properties of the $\text{Ti}(\text{OEt})_4$ catalyst and the cationic $\text{Ti}(\text{OEt})_3^+$ catalyst, the energy decomposition analyses for the transition

states **TS5** and **TS7** were performed, as shown in Table 2. The Gibbs free energy is divided into four components, namely the electronic energy E , the thermodynamic correction G_{thermo} , the solvation correction ΔG_{sol} and the contribution to the change from the standard state G_{gas} to G_{sol} . Since the contribution of the electronic energy accounts for more than 80% of the relative Gibbs free energy ΔG , the distortion–interaction model was used to systematically analyse the electronic energy and investigate how the transition state distortions and interactions control the activity of the reaction [25,26].

Table 2. Gibbs free energy decomposition analysis.

	ΔE (kcal/mol)	ΔG_{thermo} (kcal/mol)	ΔG_{sol} (kcal/mol)	ΔG_{std} (kcal/mol)	ΔG (kcal/mol)
TS5	21.3	−1.0	3.8	0.0	24.1
TS7	16.1	3.9	−0.1	0.0	19.9

In this model, the potential energy surface $\Delta E(\zeta)$ can be decomposed into two components along the reaction coordinate ζ : the distortion energy $\Delta E_{\text{dist}}(\zeta)$, which depends on the structural distortion experienced by the reactants, and the interactions between the reactants $\Delta E_{\text{int}}(\zeta)$ that result from the distortion:

$$\Delta E(\zeta) = \Delta E_{\text{dist}}(\zeta) + \Delta E_{\text{int}}(\zeta) \quad (4)$$

The transition state is divided into two parts, namely the DET molecule with $\text{Ti}(\text{OEt})_4$ or the cationic $\text{Ti}(\text{OEt})_3^+$ catalyst. The main reason for the higher energy of **TS5** than **TS7** is the high distortion energy of the DET; the C–O bond of DET extends from 1.33 Å in reactant to 2.11 Å in transition state, resulting in higher electron energy (Figure 12). The catalyst of **TS5** has a greater interaction with the DET molecule compared to **TS7** due to the shortened Ti–O bond, but it is unable to counteract its excessively high distortion energy.

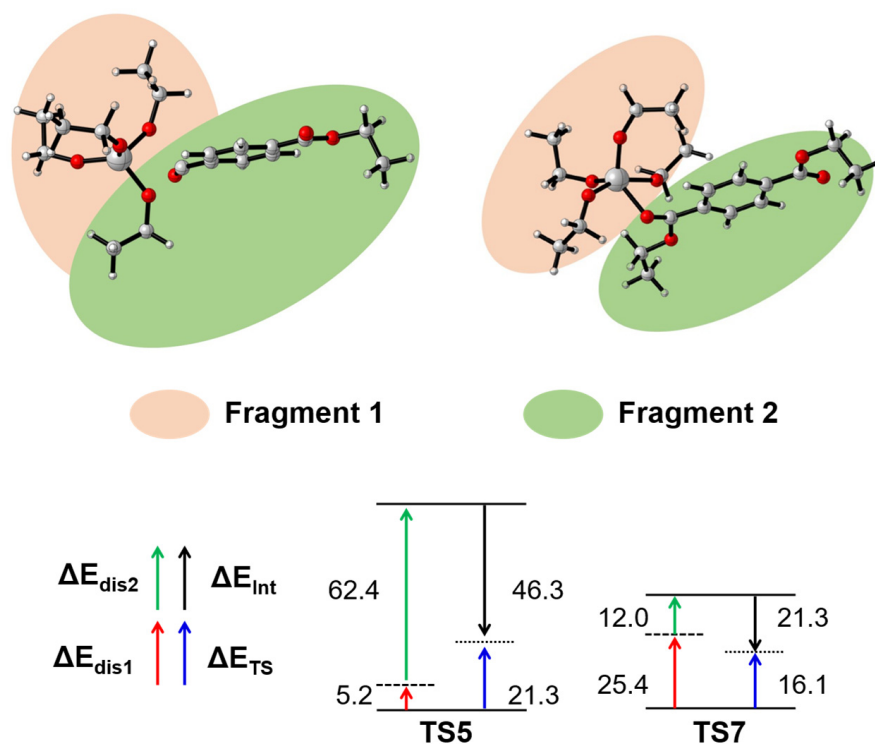


Figure 12. Distortion–interaction analysis. Fragment 1 is a Ti-catalyst and the fragment 2 is a DET molecule. ΔE_{dis1} and ΔE_{dis2} represent the distortion energy of Ti-catalyst and DET molecule, respectively. Energies are in kcal/mol.

3. Computational Details

All DFT calculations were performed using the Gaussian 09 program package [27]. The structures were fully optimized using the B3LYP-D3 function in combination with the def2-SVP basis set and the polarizable continuum model (PCM) solvation model, using 1,2-ethanediol ($\epsilon = 40.2$) as the model solvent [28–30]. The vibrational frequencies of each geometry were calculated at the same level to confirm the nature of the optimized structure. All minima on the potential energy surface showed no imaginary frequency, while the transition state only showed one imaginary frequency representing the vibrational mode in line with the corresponding reaction. To refine the electron energies (E), the large triple-zeta def2-TZVP basis set was used to perform high-level single-point energy calculations for all structures [31]. IRC calculations were performed to verify the connections between the transition state and the corresponding reactant and the product [32].

Thermochemical analysis was performed at 1 atm and 523.15 K to obtain the thermal correction of free energy (G_{therm}) [33,34]. The contribution (G_{std}) resulting from the change in the standard state from G_{gas} to G_{sol} was also included. Therefore, the relative Gibbs free energy (ΔG) is given by $\Delta G = \Delta E + \Delta G_{\text{therm}} + \Delta G_{\text{sol}} + \Delta G_{\text{std}}$. The HOMO and LUMO were calculated in the Multiwfn package and plotted using the VMD 1.9.3 program [35,36].

4. Conclusions

In order to investigate the mechanism of catalysis in the PET polycondensation reaction, DFT studies on DET molecule and Ti-based model catalysts were carried out. The possibility of cationic catalysts as catalytic active centres for polyester polycondensation reactions was examined.

In the absence of a catalyst, the transition state is a cyclic four-centred compound with an energy barrier for the transesterification reaction of DET with ethanol of 47.6 kcal/mol. Based on DFT calculations, both $\text{Ti}(\text{OEt})_4$ and cationic $\text{Ti}(\text{OEt})_3^+$ catalysts favoured the polyester polycondensation reaction, and the lowest energy barrier was found in the M3 mechanism of the $\text{Ti}(\text{OEt})_4$ catalyst (19.9 kcal/mol). Based on the distortion–interaction analysis, the $\text{Ti}(\text{OEt})_4$ catalyst was found to be superior to the $\text{Ti}(\text{OEt})_3^+$ catalyst due to the lower DET distortion energy, resulting in the largest TOF value of $3.5 \times 10^4 \text{ s}^{-1}$ in the M3 mechanism. However, this study was focused on investigating the performance of two commonly used titanium catalysts. Our forthcoming research endeavours will encompass an extensive high-throughput screening of alternative catalysts with the objective of identifying superior and more efficient options.

Supplementary Materials: The following supporting information can be downloaded at: <https://www.mdpi.com/article/10.3390/catal13101388/s1>, Figure S1: Molecular electrostatic potential (MESP) on the 0.001 a.u. electron density isosurface for the DET molecule.; Figure S2: Optimized structure of the reactant, transition state and product in M2 mechanism over $\text{Ti}(\text{OEt})_3^+$ catalyst.

Author Contributions: Z.G.: investigation, writing—original draft; J.Z.: methodology; W.Z.: review and editing; Y.Z. (Youcai Zhu): software; Z.L.: methodology, writing—review, writing—editing; Y.Z. (Yumei Zhang) and Y.Z. (Yue Zhang): project administration, writing—review, writing—editing. All authors have read and agreed to the published version of the manuscript.

Funding: This research was funded by Sinopec Scientific Research and Development Project, grant number 20/GFS21-L3-006 and the APC was funded by Sinopec.

Data Availability Statement: The data presented in this study are available on request from the corresponding author.

Acknowledgments: We acknowledge the supercomputer at SINOPEC Shanghai Research Institute of Petrochemical Technology, East China University of Science and Technology and Donghua University for generous computing resources.

Conflicts of Interest: The authors declare no conflict of interest.

References

1. Kausar, A. Review of fundamentals and applications of polyester nanocomposites filled with carbonaceous nanofillers. *J. Plast. Film. Sheeting* **2018**, *35*, 22–44. [[CrossRef](#)]
2. MacDonald, A.W. New advances in poly(ethylene terephthalate) polymerization and degradation. *Polym. Int.* **2002**, *51*, 923–930. [[CrossRef](#)]
3. Sulyman, M.; Haponiuk, J.; Formela, K. Utilization of Recycled Polyethylene Terephthalate (PET) in Engineering Materials: A Review. *Int. J. Environ. Sci. Dev.* **2016**, *7*, 100–108. [[CrossRef](#)]
4. Drault, F.; Snoussi, Y.; Thuriot-Roukos, J.; Itabaiana, I.; Paul, S.; Wojcieszak, R. Study of the Direct CO₂ Carboxylation Reaction on Supported Metal Nanoparticles. *Catalysts* **2021**, *11*, 326. [[CrossRef](#)]
5. Paparella, A.N.; Perrone, S.; Salomone, A.; Messa, F.; Cicco, L.; Capriati, V.; Perna, F.M.; Vitale, P. Use of Deep Eutectic Solvents in Plastic Depolymerization. *Catalysts* **2023**, *13*, 1035. [[CrossRef](#)]
6. Weinberger, S.; Canadell, J.; Quartinello, F.; Yeniad, B.; Arias, A.; Pellis, A.; Guebitz, G.M. Enzymatic Degradation of Poly(ethylene 2,5-furanoate) Powders and Amorphous Films. *Catalysts* **2017**, *7*, 318. [[CrossRef](#)]
7. Hua, Z.; Yue, R.; Zhenhua, L.; Ming, X.; Ye, W.; Ruixiang, G.; Xianggui, K.; Lirong, Z.; Haohong, D. Electrocatalytic upcycling of polyethylene terephthalate to commodity chemicals and H₂ fuel. *Nat. Commun.* **2021**, *12*, 4679.
8. Furukawa, M.; Kawakami, N.; Tomizawa, A.; Miyamoto, K. Efficient Degradation of Poly(ethylene terephthalate) with Thermobifida fusca Cutinase Exhibiting Improved Catalytic Activity Generated using Mutagenesis and Additive-based Approaches. *Sci. Rep.* **2019**, *9*, 16038. [[CrossRef](#)] [[PubMed](#)]
9. Sang, T.; Wallis, C.J.; Hill, G.; Britovsek, G.J.P. Polyethylene terephthalate degradation under natural and accelerated weathering conditions. *Eur. Polym. J.* **2020**, *136*, 109873. [[CrossRef](#)]
10. Punyodom, W.; Meepowpan, P.; Girdthep, S.; Limwanich, W. Influence of tin(II), aluminum(III) and titanium(IV) catalysts on the transesterification of poly(L-lactic acid). *Polym. Bull.* **2022**, *79*, 11409–11429. [[CrossRef](#)]
11. Shigemoto, I.; Kawakami, T.; Taiko, H.; Okumura, M. A quantum chemical study on the polycondensation reaction of polyesters: The mechanism of catalysis in the polycondensation reaction. *Polymer* **2011**, *52*, 3443–3450. [[CrossRef](#)]
12. Biros, S.M.; Bridgewater, B.M.; Villeges-Estrada, A.; Tanski, J.M.; Parkin, G. Antimony Ethylene Glycolate and Catecholates Compounds: Structural Characterization of Polyesterification Catalysts. *Inorg. Chem.* **2002**, *41*, 4051–4057. [[CrossRef](#)] [[PubMed](#)]
13. Le Roux, E. Recent advances on tailor-made titanium catalysts for biopolymer synthesis. *Co-ord. Chem. Rev.* **2016**, *306*, 65–85. [[CrossRef](#)]
14. Savitha, K.S.; Kumar, M.S.; Jagadish, R.L. Ti(OBu)₄/B(OBu)₃: Deciphering the mechanism for the formation of high molecular weight poly(butylene succinate). *J. Appl. Polym. Sci.* **2023**, *140*, 53842. [[CrossRef](#)]
15. Xin-Gui, L.; Ge, S.; Mei-Rong, H.; Tomoya, O.; Hiroki, Y.; Tomokazu, U.; Tomohiro, H.; Hiroshi, I. Cleaner synthesis and systematic characterization of sustainable poly(isosorbide-co-ethylene terephthalate) by environment-benign and highly active catalysts. *J. Clean. Prod.* **2019**, *206*, 483–497.
16. Shen, J.; Gao, X.; Liu, Z.; Zhao, L.; Xi, Z.; Yuan, W. Reaction mechanism study on transesterification in synthesis of thermotropic liquid crystalline polymer catalyzed by zinc(II) carboxylate: A combination of DFT and kinetics analyses. *Chem. Eng. J.* **2022**, *446*, 136848. [[CrossRef](#)]
17. Huang, J.; Meng, H.; Luo, X.; Mu, X.; Xu, W.; Jin, L.; Lai, B. Insights into the thermal degradation mechanisms of polyethylene terephthalate dimer using DFT method. *Chemosphere* **2022**, *291*, 133112. [[CrossRef](#)] [[PubMed](#)]
18. Shigemoto, I.; Kawakami, T.; Okumura, M. A quantum chemical study on polymerization catalysts for polyesters: Catalytic performance of chelated complexes of titanium. *Polymer* **2013**, *54*, 3297–3305. [[CrossRef](#)]
19. Wang, J.; Zhang, S.; Han, Y.; Zhang, L.; Wang, Q.; Wang, G.; Zhang, X. UiO-66(Zr/Ti) for catalytic PET polycondensation. *Mol. Catal.* **2022**, *532*, 112741. [[CrossRef](#)]
20. Wolzak, L.A.; van der Vlugt, J.I.; Berg, K.J.v.D.; Reek, J.N.H.; Tromp, M.; Korstanje, T.J. Titanium-catalyzed esterification reactions: Beyond Lewis acidity. *ChemCatChem* **2020**, *12*, 5229–5235. [[CrossRef](#)]
21. Zhang, J.; Guan, Z.; Zhu, Y.; Liu, Z. DFT Study on the Mechanism of Thermal Degradation of Polyester. *J. Mol. Catal.* **2022**, *36*, 425–432. [[CrossRef](#)]
22. Ahmadnian, F.; Velasquez, F.; Reichert, K.-H. Screening of Different Titanium (IV) Catalysts in the Synthesis of Poly(ethylene terephthalate). *Macromol. React. Eng.* **2008**, *2*, 513–521. [[CrossRef](#)]
23. Siling, M.I.; Laricheva, T.N. Titanium compounds as catalysts for esterification and transesterification. *Russ. Chem. Rev.* **1996**, *65*, 279–286. [[CrossRef](#)]
24. Kozuch, S. Steady State Kinetics of Any Catalytic Network: Graph Theory, the Energy Span Model, the Analogy between Catalysis and Electrical Circuits, and the Meaning of “Mechanism”. *ACS Catal.* **2015**, *5*, 5242–5255. [[CrossRef](#)]
25. Paton, R.S.; Kim, S.; Ross, A.G.; Danishefsky, S.J.; Houk, K.N. Experimental Diels-Alder Reactivities of Cycloalkenones and Cyclic Dienes Explained through Transition-State Distortion Energies. *Angew. Chem. Int. Ed.* **2011**, *50*, 10366–10368. [[CrossRef](#)]
26. Fernández, I.; Bickelhaupt, F.M. The activation strain model and molecular orbital theory: Understanding and designing chemical reactions. *Chem. Soc. Rev.* **2014**, *43*, 4953–4967. [[CrossRef](#)] [[PubMed](#)]
27. Frisch, M.J.; Trucks, G.W.; Schlegel, H.B.; Scuseria, G.E.; Robb, M.A.; Cheeseman, J.R.; Scalmani, G.; Barone, V.; Mennucci, B.; Petersson, G.A.; et al. *Gaussian 09, Revision, E.01*; Gaussian Inc.: Wallingford, CT, USA, 2009.

28. Tomasi, J.; Mennucci, B.; Cammi, R. Quantum Mechanical Continuum Solvation Models. *Chem. Rev.* **2005**, *105*, 2999–3094. [[CrossRef](#)] [[PubMed](#)]
29. Grimme, S.; Antony, J.; Ehrlich, S.; Krieg, H. A consistent and accurate ab initio parametrization of density functional dispersion correction (DFT-D) for the 94 elements H-Pu. *J. Chem. Phys.* **2010**, *132*, 154104–154119. [[CrossRef](#)] [[PubMed](#)]
30. Brandenburg, J.G.; Grimme, S. Dispersion corrected hartree-fock and density functional theory for organic crystal structure prediction. *Top Curr. Chem.* **2014**, *345*, 1–23. [[PubMed](#)]
31. Xu, X.; Truhlar, D.G. Accuracy of Effective Core Potentials and Basis Sets for Density Functional Calculations, Including Relativistic Effects, As Illustrated by Calculations on Arsenic Compounds. *J. Chem. Theory Comput.* **2011**, *7*, 2766–2779. [[CrossRef](#)] [[PubMed](#)]
32. Fukui, K. The path of chemical reactions-the IRC approach. *Accounts Chem. Res.* **1981**, *14*, 363–368. [[CrossRef](#)]
33. Becke, A.D. A new mixing of Hartree-Fock and local density-functional theories. *J. Chem. Phys.* **1993**, *98*, 1372–1377. [[CrossRef](#)]
34. Lee, C.; Yang, W.; Parr, R.G. Development of the Colle-Salvetti correlation-energy formula into a functional of the electron density. *Phys. Rev. B* **1988**, *37*, 785–789. [[CrossRef](#)] [[PubMed](#)]
35. Lu, T.; Chen, F. Multiwfn: A multifunctional wavefunction analyzer. *J. Comput. Chem.* **2012**, *33*, 580–592. [[CrossRef](#)] [[PubMed](#)]
36. Humphrey, W.; Dalke, A.; Schulten, K. VMD: Visual molecular dynamics. *J. Mol. Graph.* **1996**, *14*, 33–38. [[CrossRef](#)] [[PubMed](#)]

Disclaimer/Publisher’s Note: The statements, opinions and data contained in all publications are solely those of the individual author(s) and contributor(s) and not of MDPI and/or the editor(s). MDPI and/or the editor(s) disclaim responsibility for any injury to people or property resulting from any ideas, methods, instructions or products referred to in the content.